Minimizing the PAPR for FBMC/OQAM Signals Using Enhanced-PTS with Low Complexity Search

Mahaman Noura Issaka Ango[1], Elijah Mwangi[2], and Moctar Mossi Idrissa[3]
[1] Department of Electrical Engineering, Pan African University, P.O. BOX 62000 Nairobi, Kenya
[2] Faculty of Engineering, University of Nairobi, P.O. BOX 30197 Nairobi, Kenya
[3] Department of Physics, Université Abdou Moumouni de Niamey, P.O. BOX 10662 Niamey, Niger
Email: nouraango1992@gmail.com; mwangiel2010@gmail.com; mmoctar@gmail.com

Abstract—The filter bank multicarrier with offset quadrature amplitude modulation (FBMC/OQAM) scheme has recently become a focus of interest for many scholars and researchers. Despite its impressive advantages over Orthogonal Frequency Division Multiplexing (OFDM), the FBMC/OQAM system exhibits high Peak-to-Average Power Ratio (PAPR) which could plague its performance if it is not properly managed. In this paper, we proposed a PAPR reduction scheme that improves the Partial Transmit Sequence (PTS) to an enhanced PTS (EPTS), then employs a low complexity search to determine the optimal combination of phase factors. In the enhanced PTS, the FBMC/OQAM data blocks are partitioned into sub-blocks by taking into account their overlapping arrangement, then a segmentation operation is performed to the overall overlapping partitioned data blocks in order to form several segments of sub-blocks. After that, the segments are optimized consecutively by applying a phase factor search approach. Referred to as enhanced PTS with iterative flipping (EPTS-IF), the proposed scheme optimizes consecutively the segments of sub-blocks by employing Iterative Flipping approach. The PAPR reduction performance and the computational complexity of the proposed scheme have been evaluated through computer simulations and theoretical analysis which revealed a significant PAPR reduction gain of approximately 30.48%, and at a low computational cost.

Index Terms—Enhanced-PTS, FBMC/OQAM, Iterative Flipping (IF), Low Complexity, PAPR

I. Introduction

Recently, the gradual growth of societal needs has imposed several technical challenges that need to be addressed to adequately fulfil the stringent consumer requirements for wireless communication services, including massive device connectivity, very high spectral and energy efficiency, extremely high achievable data rate, high throughput, near-zero latency, and very high reliability. To address these challenges, the 5G technology is continuously being deployed in many parts of the world [1]. Most of the current wireless communication systems employ multicarrier modulation (MCM) technology due to the potential in providing high data rate transmission and its flexibility in the frequency-selective channels. Among the widely-applied MCM schemes, orthogonal frequency division multiplexing (OFDM) has been popular in digital communication systems, exclusively in long term evolution standard (4G-LTE), and recently adopted as the physical layer of 5G New Radio (5G-NR). However, compared to some recent modulation schemes, the OFDM scheme suffers from large out-of-band (OOB) signal emission, and exhibits a restricted spectral efficiency due to the use of Cyclic Prefix (CP) in its symbols. Furthermore, due to its high sensitivity to timing errors, OFDM scheme becomes less robust in handling huge synchronization scenarios that mostly occurs in massive machine-type communication (mMTC).

Lately, the FBMC/OQAM technique has been a focus of interest to many researchers as an alternative to OFDM and also an appropriate contender for cognitive radio applications [2]. Although FBMC/OQAM modulation is not used in the 5G mobile communication systems, its impressive features cannot be neglected since it may play a key role as an air interface for the communication technologies beyond 5G [3]. Compared to OFDM, the FBMC/OQAM systems possess some outstanding features such as high spectral efficiency since it does not involve the CP, attractive time-frequency localization property, pulse shaping, and poor OOB leakage [4], [5]. However, despite its potential merits, large PAPR plagues FBMC/OQAM system. When a FBMC/OQAM signal with high peak goes through a high-power amplifier (HPA) with poor dynamic range, unwanted effects such as in-band distortion and OOB radiation may emerge; thus, causing Adjacent Channel Interference (ACI) [6]. In addition, the former effects may also result in bit error rate (BER) degradation of the system. HPAs with high back-off power are the most suitable technology to accommodate signals with high PAPR, but at the expense of energy efficiency. In this regard, in order to fulfill the requirement of future communication systems in terms of energy efficiency it could be economically advantageous to mitigate the issue of large PAPR at the transmitter rather than employing the costly HPAs.

Over the recent years, significant efforts have been made by many researchers in proposing numerous techniques to resolve the problem of inherent high PAPR in OFDM. In the literature, the PAPR reduction algorithms are assorted into two main groups [7]. The first category is

Manuscript received November 25, 2021; revised May 15, 2022.
Corresponding author email: nouraango1992@gmail.com.
doi:10.12720/jcm.17.6.412-422

made up of signal distortion schemes among which the most popular are active constellation extension (ACE) [8], clipping [9], clipping and filtering [10], nonlinear companding transform [11], and peak windowing [12]. The second class consists of signal distortionless techniques such as block coding [13], selective mapping (SLM) [14], partial transmit sequence (PTS) [15], [16], and Tone Reservation (TR) [17].

Nevertheless, in an FBMC/OQAM system, multiple data blocks overlap with each other while symbols are independent in OFDM system. Accordingly, most of the ordinary PAPR reduction schemes for OFDM cannot mitigate efficiently the problem of high PAPR in FBMC/OQAM system. For this reason, several works have proposed new approaches to efficiently overcome the high peak signals in FBMC/OQAM system.

In [1], the authors presented a hybrid scheme based SLM and PTS for PAPR reduction in FBMC/OQAM systems. The overlapping impact of multiple data blocks was taken into account, and an artificial bee colony algorithm was employed to overcome the computational complexity that arises from the joint method.

In 2019, Ikni *et al.* [18] introduced a new scheme which considered the overlapping nature of FBMC/OQAM symbols in the decrease of the instantaneous power fluctuation of FBMC/OQAM signal envelope. Referred to as discrete sliding norm transform, the proposed technique was developed based on L_2-metric and the norm of five samples at every sliding process. No side information was required at the receiver side, and significant PAPR reduction was attained with low computational complexity in the proposed scheme. However, more improvement in terms of PAPR reduction is still needed.

Senhadji *et al*. [19] associated a conventional TR scheme with deep clipping technique in order to cancel the peaks of FBMC/OQAM signals without degrading the BER performance of the system. Satisfactory improvement was achieved in terms of PAPR reduction performance, but the proposed scheme did not take into account the overlapping of FBMC/OQAM signals.

In [20], a hybrid peak power reduction scheme based on SLM and multi-data block PTS (M-PTS) algorithms was presented. Firstly, the proposed method processed the data block signal by employing the SLM scheme. Then, it was segmented into multiple portions of several data blocks which were later optimized gradually with consideration of the overlaping effect of the previous data blocks.

On the other hand, Kumar [21] investigated the reduction of PAPR in FBMC/OQAM signals by combining iterative filtering and an efficient companding transform methods. The proposed algorithm did not suffer from OOB radiation and showed effectiveness in terms of PAPR reduction with a reasonable computational complexity.

Another upgraded PTS-based method was proposed in [22] with the purpose of overcoming the excessive PAPR in FBMC/OQAM signals. Although the proposed method minimizes significantly the peak power, its complexity was not improved. The authors in [23] presented an improved PTS-based scheme which employed two-steps PAPR minimization for FBMC/OQAM signals. The proposed scheme yielded significant PAPR suppression performance, with reduced computational complexity. Nevertheless, this scheme employed exhaustive searches recognizing that its complexity would increase exponentially with the growth of subblock's size.

Segment-based optimization technique employing a restricted number of phase factors sets was presented in [24]. This method minimizes the PAPR in three-steps such as minimization of peaks power, optimization of phase factors, and clipping. Alternatively, Merah *et al*. [25] presented an PTS-based approach which took into consideration the overlapping of FBMC signals, and overcame the need of using additional bits to send the side information (SI). These techniques maintained satisfactory BER and showed substantial PAPR reduction achievement with low complexity.

To suppress the large PAPR of FBMC-OQAM signals, authors in [26], suggested a novel scheme called conversion vector-based low-complexity dispersive selection mapping (C-DSLM). In this proposed algorithm, the candidate signals were engendered by multiplying the original FBMC signal by the cyclic shift of a well-designed set of conversion vectors with large number of zero elements. The PAPR reduction achievement of the C-DSLM method is comparable to that of the DSLM algorithm, and a very low computational complexity was achieved.

Authors in [27] introduced a method termed the genetic algorithm based bilayer PTS (GA-BPTS) for peak power cancellation in FBMC/OQAM signals. The GA-BPTS operated on two layers of PTS scheme. Although low computational complexity was achieved, the PAPR reduction performance was not significant.

In this paper, we present an enhanced PTS scheme which employs iterative flipping (IF) [7] as an optimization approach. This scheme is developed with the aim of decreasing the large PAPR for the FBMC/OQAM signals, and maintaining a low level of computational complexity. The proposed method takes into account the overlaps of FBMC/OQAM signals and operates in two main stages. In the first stage, is performed the partition of the FBMC/OQAM data blocks into a defined number of sub-blocks which are buffered with consideration of the overlap between consecutive symbols. Then the FBMC data blocks are partitioned into multiple segments of sub-blocks to avoid the peak power re-growth. In the second stage, an optimization process is carried out in each segment of a sub-block by applying the aforementioned phase search approach. Substantial improvements in terms of PAPR and computational complexity reductions are achieved in the proposed method.

The remainder of the paper is arranged as follows: Section II introduces the FBMC/OQAM transmitter model and the PAPR of the signals. The conventional and the proposed PAPR mitigation scheme are discussed in

Section III. The simulation results are shown and discussed in Section IV. Lastly, Section V draws the conclusions.

II. FBMC/OQAM System Model

A. FBMC/OQAM System

The block structure of FBMC/OQAM transmitter where M blocks of data are consecutively sent over N parallel subchannels is illustrated in Fig. 1. The m^{th} input data block vector can be defined as:

$$X^m = \left[X_1^m, X_2^m, \ldots, X_N^m \right]^T \tag{1}$$

where $[\cdot]^T$ and X_k^m denote the transpose, and the m^{th} complex input symbol on the k^{th} subcarrier, respectively. The complex symbol X_k^m can be given as:

$$X_k^m = a_k^m + jb_k^m \tag{2}$$

where, $a_k^m = \Re\{X_k^m\}$ *and* $b_k^m = \Im\{X_k^m\}$. $\Re\{\cdot\}$ and $\Im\{\cdot\}$ stand for the real and imaginary components of a symbol, respectivily. k and m denote the subcarrier and data block indexes, respectively, with range defined as $1 \le k \le N$ and $1 \le m \le M$. The symbol N is the subcarrier's number and M is the number of data blocks.

Thus, the data matrix X representing the M complex-valued input data block can be expressed as:

$$X = \left[X^1, X^2, \ldots, X^m, \ldots, X^M \right] \tag{3}$$

In the OQAM pre-processing, a staggering operation is performed on each X_k^m components where, the real and imaginary parts are interleaved by $T/2$ in order to form OQAM symbols, where T is the time duration of a block. Subsequently, the OQAM symbols are processed by a bank of filters and then modulated with N orthogonal subchannels to achieve the modulated OQAM symbols. Thus, the m^{th} transmitted FBMC/OQAM data block is achieved by summing up over all the N subcarriers of the modulated symbols. Equation (4) gives the time-domain expression of the m^{th} FBMC-OQAM data block signal [18], [19], [28].

$$S^m(t) = \sum_{k=1}^{N} \left[a_k^m h\left(t-(m-1)T\right) + jb_k^m h\left(t-(m-1)T-\frac{T}{2}\right) \right] e^{j(k-1)\varphi_t},$$
$$(m-1)T \le t \le \left(m+K-\frac{1}{2}\right)T. \tag{4}$$

where, $\varphi_t = \left(\frac{2\pi t}{T} + \frac{\pi}{2}\right)$ and $h(t)$ represent the phase term and the impulse response of the prototype filter, respectively.

The time-domain of the output FBMC/OQAM signal $S(t)$ is formed by adding up all the M FBMC data blocks as given in equation (5):

$$S(t) = \sum_{m=1}^{M} \sum_{k=1}^{N} \left[a_k^m h\left(t-(m-1)T\right) + jb_k^m h\left(t-(m-1)T-\frac{T}{2}\right) \right] e^{j(k-1)\varphi_t},$$
$$0 \le t \le \left(M+K-\frac{1}{2}\right)T. \tag{5}$$

Fig. 2 illustrates the behaviour of the physical layer for dynamic spectrum access and cognitive radio (PHYDYAS) filter compared to the well-known rectangular pulse in frequency domain. It is explicit that the PHYDYAS filter with an overlapping value $K = 4$ achieves a higher side-band suppression. Therefore, in this research investigation the PHYDYAS filter [29] is adopted as default prototype filter. Furthermore, in view of the prototype filter's time duration, and the staggering between real and imaginary components of each FBMC symbol, it is obvious that adjacent data blocks overlap. Thus, each processed data block has a length of $(K + 1/2)T$, and the overall time duration of the desired time-domain FBMC/OQAM signal is $(K + M - 1/2)T$.

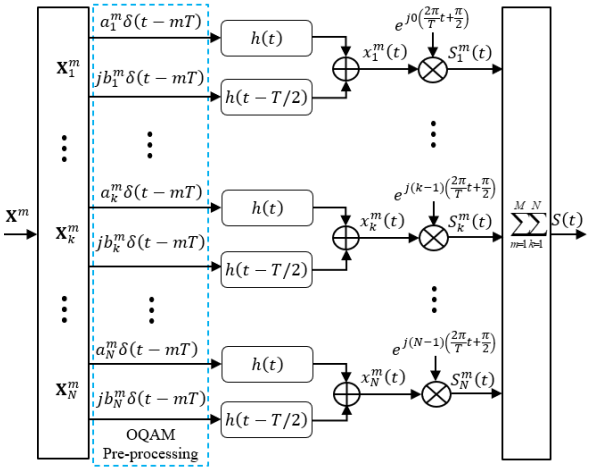

Fig. 1. Structure of FBMC/OQAM transmitter

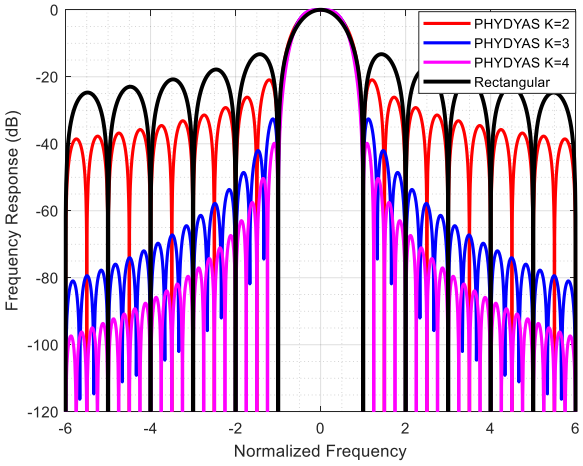

Fig. 2. Frequency Response of PHYDYAS and Rectangular pulse

B. PAPR of FBMC/OQAM Signals

The PAPR reduction technique is implemented for discrete-time domain signals. Thus, the FBMC/OQAM

signal is converted to the discrete-time domain through the sampling process, where T/F characterizes the sampling period, with $F = LN$, and L the oversampling factor. Thus, the discrete-time expression of the modulated FBMC/OQAM signal at sample n is given by equation (6).

$$S[n] = \sum_{m=1}^{M}\sum_{k=1}^{N}\left[a_k^m h\left(n-(m-1)F\right) + jb_k^m h\left(n-(m-1)F-\frac{F}{2}\right)\right]e^{j(k-1)\varphi_n}, \quad 1 \le n \le (M+K)F \tag{6}$$

where $h[n]$ denotes the discrete sequence filter, designed based on frequency sampling technique; hence implemented as a discrete time filter. The impulse response expression of PHYDYAS filter is given in equation (7).

$$h(t) = H_0 + 2\sum_{k=1}^{K}(-1)^k H_k cos\left(2\pi\frac{k}{KT}t\right), \quad t \in [0,\ KT] \tag{7}$$

Applying the Nyquist sampling rate to $h(t)$ yields the discrete-time formulation of the PHYDYAS as:

$$h[n] = 1 + 2\sum_{k=1}^{K}(-1)^k H_k cos\left(2\pi\frac{k}{KN}n\right), \quad n = 1,\ldots,L_p \tag{8}$$

where H_k denotes the filter coefficients given as [29]:

$$\begin{aligned} H_0 &= 1, & H_1 &= 0.971960 \\ H_2 &= 0.707106, & H_3 &= 0.235147 \end{aligned} \tag{9}$$

The PAPR of the FBMC/OQAM signal with *M* data blocks can be evaluated by dividing the output sequence, $S[n]$ into $(M+K)$ consecutive signal segments, each with length equivalent to *F* samples. Consequently, the PAPR in the j^{th} segment can be estimated as shown in equation (10).

$$PAPR_j = \frac{\max\limits_{(j-1)F+1 \le n \le jF}\left|S[n]\right|^2}{E\left[\left|S[n]\right|^2\right]}, \quad 1 \le j \le M+K \tag{10}$$

where $E[\cdot]$ is the expectation operator, and $\max\limits_n |S[n]|^2$ is the peak power (P_j) in the j^{th} segment.

To evaluate how recurrent the PAPR of the signal exceeds a defined threshold ($PAPR_{TH}$), complementary cumulative distribution function (CCDF) is employed, as given [30]:

$$CCDF\left(PAPR > PAPR_{TH}\right) = \frac{1}{(M+K)I}\sum_{i=1}^{I}\sum_{j=1}^{M+K}\eta_{j,i} \tag{11}$$

where *I* is the number of tests for the simulation, and

$$\eta_{j,i} = \begin{cases} 1, & if\ PAPR_j\ and\ i^{th}\ test > PAPR_{TH} \\ 0, & elsewhere \end{cases} \tag{12}$$

III. PAPR Reduction Techniques

A. Conventional PTS Method

The main idea in the PTS scheme is to mitigate the peak signals by scrambling the input data block with the optimum phase weighting factors.

In the OFDM system, the conventional PTS (C-PTS) algorithm operates by first dividing the m^{th} input data block X^m into *V* disjoint sub-blocks denoted $X^{m,v}$ such as $X^m = \sum_{v=1}^{V} X^{m,v}$. After that, the sub-blocks are converted into the time-domain, then multiplied by the phase factors, and lastly combined to form a set of candidate signals from which the signal with the lowest PAPR is selected for transmission.

Likewise, in the FBMC/OQAM system, a data block undergoes a partition process as described below:
Let us express a vector sequence in the m^{th} data block as:

$$S^m[n] = \left(S_1^m[n], S_2^m[n], \ldots, S_k^m[n], \ldots, S_N^m[n]\right)^T \tag{13}$$

i. Divide the vector sequence $S^m[n]$ into *V* sub-blocks. Thus, the vector sequence of the v^{th} sub-block located in the m^{th} data block is expressed as:

$$S^{m,v}[n] = \left(S_1^{m,v}[n], \ldots, S_k^{m,v}[n], \ldots, S_N^{m,v}[n]\right) \tag{14}$$

where,

$$S_k^{m,v}[n] = \begin{cases} S_k^m[n], & if\ S_k^m[n] \in v^{th}\ subblock \\ 0, & \text{otherwise} \end{cases} \tag{15}$$

ii. Sum up all the samples in the v^{th} subblock, so as to form the v^{th} subblock's signal in the m^{th} data block.

$$\tilde{S}^{m,v}[n] = \sum_{k=1}^{N} S_k^{m,v}[n] \tag{16}$$

Consequently, each FBMC/OQAM data block will yield *V* sub-blocks of signals.

Following the partition process, each sub-block $\tilde{S}^{m,v}[n]$ is multiplied by a weighting phase factor $\psi^{m,v}$ selected from a W-element set, Ψ^m and then summed up together to generate a candidate signal expressed as:

$$\breve{S}^m[n] = \sum_{v=1}^{V}\psi^{m,v}\tilde{S}^{m,v}[n] \tag{17}$$

$\Psi^m = \left\{\psi^{m,v} = e^{j\frac{2\pi i}{W}}, i = 0,1,\ldots,W-1\right\}$, where *W* represents the number of allowed values of phase rotation factors.

Thus, the PAPR in the m^{th} data block signal can be minimized by choosing the optimum phase weighting factor sequence Ψ_{opt}^m that leads to the signal with the lowest peak power. Ψ_{opt}^m can be given as:

$$\Psi_{opt}^m = \underset{\left[\psi^{m,1},\psi^{m,2},\ldots,\psi^{m,V}\right]}{arg\ min}\left\{\max_n\left|S[n]\right|^2\right\} \tag{18}$$

where $\Psi_{opt}^{m} = \left[\psi_{opt}^{m,1}, \psi_{opt}^{m,2}, \ldots, \psi_{opt}^{m,V}\right]$ is the solution to (18) achievable after W^V trials of various phase factor vectors. The optimal m^{th} FBMC data block signal is stated as:

$$\breve{S}_{opt}^{m}[n] = \sum_{v=1}^{V} \psi_{opt}^{m,v} \tilde{S}^{m,v}[n] \quad (19)$$

Eventually, the discrete-time domain FBMC/OQAM output signal with the reduced peak power is obtained by adding together the optimal signals of all data blocks.

$$\breve{S}_{opt}[n] = \sum_{m=1}^{M} \breve{S}_{opt}^{m}[n], \quad 1 \le n \le \left(M + K - \frac{1}{2}\right). \quad (20)$$

Clearly, the aforementioned steps outline how the C-PTS algorithm can be employed to handle the peak power drawbacks in the FBMC/OQAM signals by individually processing the data blocks as for the OFDM signals.

B. Proposed PAPR Reduction Scheme

This subsection outlines the working process of the proposed PAPR reduction scheme. The first two working steps of the proposed algorithm focus in building up the segments of FBMC/OQAM signal sub-blocks, termed as EPTS. Initially, the first FBMC/OQAM data block undergoes partition operation as performed in the C-PTS (see subsection A) so as to form V sub-blocks of signals, each with length of $(K + 1/2)F$, referred to as block of sub-blocks which is later buffered. Subsequently, the partition process is also applied to the second FBMC data block. Afterwards, the result block of sub-blocks is added to the portion of the previous block that overlaps it, and lastly buffered following the non-overlapping part of the preceding block. Similar operations in the second data block are carried out in the third discrete-time FBMC/OQAM data block, then the result block of sub-blocks is as well buffered succeeding the non-overlapping portion of the former block. The processes are repeated for the fourth FBMC data block and so on until all the data blocks are handled this way. Eventually, a block of V FBMC/OQAM sub-blocks is achieved, with a length designated by $(K + M - 1/2)F$ samples. In the second step, the block of sub-blocks is split into $(M + K)$ signal segments, each of length F. Accordingly, the overlapping property of the FBMC data blocks are taken into account in the composition of block of sub-blocks, and segmentation is performed so as to boost the minimization of signal peaks and avoid the spectral re-growth. The candidate signals in each segment are achieved by applying the iterative flipping as a phase factor's search strategy. Consequently, the use of this approach to optimizing the segments of signal sub-blocks yields the enhanced PTS with iterative flipping (EPTS-IF) as the proposed PAPR reduction scheme.

The EPTS-IF scheme optimizes consecutively the segments of sub-blocks by employing iterative flipping.

An outline of the steps involved in the EPTS-IF are given below.

Step i: Building up a block of V FBMC/OQAM sub-blocks signals by dividing and buffering consecutively the M FBMC discrete-time data blocks. To that end, a block of V overlapping OQAM-FBMC sub-blocks with a length of $(K + M - 1/2)F$ is achieved, and $\hat{S}^{v}[n]$ denotes the v^{th} sub-block's sequence in that block.

$$\hat{S}^{v}[n] = \sum_{m=1}^{M} \tilde{S}^{m,v}[n] \quad (21)$$

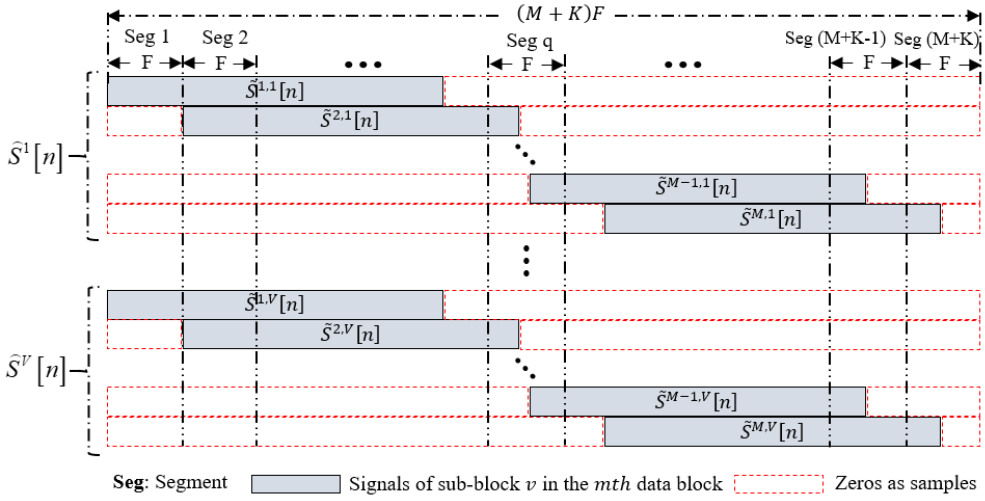

Fig. 3. Segmented sub-blocks of signals in the Enhanced-PTS scheme

Step ii: Split the block obtained in step i into $(M + K)$ segments of V consecutive FBMC/OQAM sub-blocks, each with a length of F. Here, $\hat{S}_{q}^{v}[n]$ denotes the v^{th} subblock's sequence in the q^{th} segment. Fig. 3 illustrates the segmented block of FBMC/OQAM sub-blocks.

Step iii: For $q = 1$, initialize the phase factor vector (i.e., set $\psi^{q,v} = 1$, for $v = 1, 2, \ldots, V$). Then, evaluate the $PAPR_q$ of $S_q[n]$, the combined sequence in the q^{th} segment and name it $PAPR_{min}$. Thus, a candidate signal for the q^{th} segment is given as:

$$\hat{S}_q[n]=\sum_{v=1}^{V}\psi^{q,v}\hat{S}_q^v[n],\quad (q-1)F+1\le n\le qF \quad (22)$$

where $\psi^{q,v}\in\left\{e^{j2\pi i/W},\ i=0,1,\ldots,W-1\right\}$.

Step iv: Invert the first phase factor ($v=1$) $\psi^{q,1}=-1$ and recalculate the new $PAPR_q$ of $S_q[n]$. If the new $PAPR_q > PAPR_{min}$, switch $\psi^{q,1}$ to its previous value; otherwise retain $\psi^{q,1}=-1$ and update $PAPR_q = PAPR_{min}$

Step v: Repeat step iv for $v=2$ and so on until all the possibilities for switching the phase factor's signs are explored (i.e., $v=V$). Thus, the optimum phase factor vector for the q^{th} segment is given by equation (23).

$$\Psi_{opt}^{q}=\underset{\left[\psi^{q,1},\psi^{q,2},\ldots,\psi^{q,V}\right]}{arg\ min}\left\{\max_{n}\left|\hat{S}_q[n]\right|^2\right\}. \quad (23)$$

where $\Psi_{opt}^{q}=\left[\psi_{opt}^{q,1},\psi_{opt}^{q,2},\ldots,\psi_{opt}^{q,V}\right]$.

Step vi: Compute the optimum candidate sequence for the q^{th} segment as given in (24).

$$\hat{S}_q^{opt}[n]=\sum_{v=1}^{V}\psi_{opt}^{q,v}\hat{S}_q^v[n]. \quad (24)$$

Step vii: Set $q=2$, then repeat steps (iii) to (vi), and so on until all the segments are processed that way.

In conclusion, the optimal FBMC/OQAM output signal is a sequence of $(M+K)$ consecutive signal segments with minimized PAPR. The symbol, $\hat{S}^{opt}[n]$ denotes the optimal discrete-time FBMC/OQAM sequence.

C. Computational Complexity Analysis

One of the common constraints for practical implementation of many PAPR reduction methods is the computational cost. In this paper, we estimated the computational complexity of the C-PTS, Iterative Flipping PTS (I-PTS) [7] and the proposed EPTS-IF schemes in terms of number of real multiplications and real additions necessary to achieve the optimum set of phase factors. Furthermore, we recall that one complex addition is identical to 2 real additions, and one complex multiplication corresponds to 4 real multiplications and 2 real additions.

Without any loss of performance, we set to 1 the phase factor of the first sub-block in the C-PTS scheme. Thus, employing the C-PTS algorithm to a single FBMC data block signal involves W^{V-1} tests of different combinations of phase factor so as to achieve the optimal candidate sequence. Since every single data block has a length of $F(K+1/2)$, each candidate phase factor combination will imply $VF(K+1/2)$ and $F(V-1)(K+1/2)$ complex multiplications and complex additions, respectively. Thus, $VFW^{V-1}(K+1/2)$ complex multiplications, and $FW^{V-1}(V-1)(K+1/2)$ complex additions are needed to process each FBMC data block signal. Eventually, the number of real multiplications and real additions involved by M data blocks in the C-PTS are given Table I.

For the I-PTS scheme, only V combinations of phase rotation factors necessitate to be explored in order to build all the possible candidate signals for each data block. This means, in each data block $VFV(K+1/2)$ complex multiplications, and $FV(V-1)(K+1/2)$ complex additions are involved for achieving the optimal candidate sequence. Similar to the previous analysis, M data blocks are processed this way, and the overall number of real multiplications and real additions are provided in Table I.

On the other hand, in the proposed EPTS-IF method, the search of optimal phase factors sequence is performed over V combinations of phase weighting factors. Thus, knowing that the segments are equal in length of F, every single combination of phase factor will involve VF complex multiplications, and $(V-1)F$ complex additions. This means, VVF complex multiplications and $V(V-1)F$ complex additions are required to test all the V combinations of phase factors. Consequently, the total number of operations indispensable to handle $(M+K)$ segments are summarized in Table I.

TABLE I: COMPLEXITY OF THE EPTS-IF, I-PTS, AND C-PTS ALGORITHMS

Method	Real multiplications	Real additions
EPTS-IF	$4V^2F(M+K)$	$4VF(M+K)\left(V-\frac{1}{2}\right)$
I-PTS	$4MFV^2\left(K+\frac{1}{2}\right)$	$4MFV\left(K+\frac{1}{2}\right)\left(V-\frac{1}{2}\right)$
C-PTS	$4MVFW^{V-1}\left(K+\frac{1}{2}\right)$	$4MFW^{V-1}\left(K+\frac{1}{2}\right)\left(V-\frac{1}{2}\right)$

IV. SIMULATION RESULTS AND DISCUSSION

In this section, extensive simulations were done to evaluate the PAPR reduction achievement of the proposed EPTS-IF technique compared to the C-PTS and I-PTS schemes. The PHYDYAS filter with length of $L_p=KLN$ is employed as default filter. The number of allowed phase factors is set to $W=2$ which means all the phase rotation factors are chosen from $\{+1,-1\}$. Besides, adjacent partition is used as sub-block partitioning approach. The PAPR is quantified using CCDF. The complete values of the simulation parameters are provided in Table II.

TABLE II: SIMULATION PARAMETERS

Parameters	Value
Technique	FBMC/OQAM
Number of subcarriers (N)	64
Number of data blocks (M)	16
Modulation scheme	4OQAM
Overlapping factor (K)	4
Oversampling factor (L)	4
Number of subblocks	4, 8, 16

A. Simulation Results

The CCDF vs PAPR performance of the C-PTS scheme under 4-OQAM modulation order, $N = 64$ subcarriers, and varying number of sub-blocks is illustrated is Fig. 4. In this case, the C-PTS scheme was directly employed to the FBMC/OQAM, and the PAPRs of the signal at CCDF of 10^{-3} are 10.5 dB, 10.2 dB, 9.8 dB, 9.4 dB, and 9.0 dB for the FBMC/OQAM signal, and the C-PTS when $V = 2, 4, 8$, and 16 sub-blocks, respectively. It is evident that the value of PAPR decreases as the number of sub-blocks increases. However, the C-PTS does not handle appropriately the large amount of PAPR in FBMC/OQAM signal because although the use of large number of subblocks ($V = 16$) a gain of only 1.5 dB was achieved. This confirms that the direct use of PTS-based schemes in the FBMC/OQAM signal does not yield a consequential PAPR reduction. Furthermore, exponential computational complexity occurs in the C-PTS due of exhaustive search of phase rotation factors.

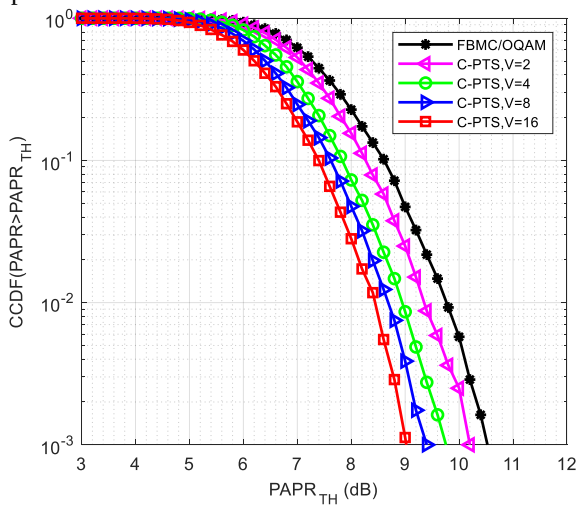

Fig. 4. CCDF vs PAPR performance of FBMC/OQAM signal with C-PTS scheme when $V = 2, 4, 8$, and 16.

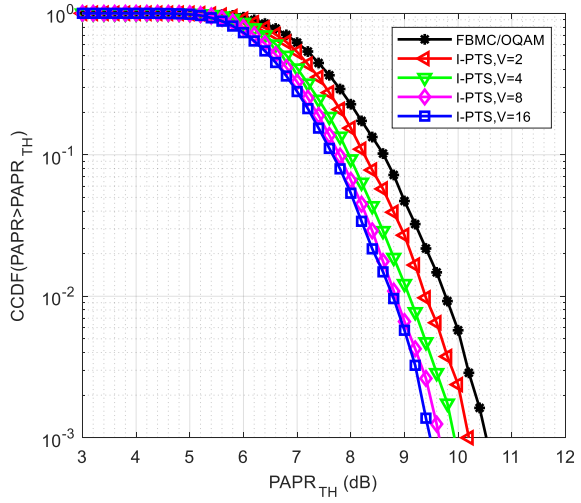

Fig. 5. CCDF vs PAPR performance of FBMC/OQAM signal with Iterative-PTS scheme when $V = 2, 4, 8$, and 16.

In Fig. 5, the PAPR reduction performance of the Iterative Flipping PTS (I-PTS) approach directly employed to the FBMC/OQAM signal was evaluated. Similar to the C-PTS, 4-OQAM modulation scheme, 64 subcarriers, and different number of sub-blocks in a range of 2 to 16 were employed in the simulation. For $V = 2$, the PAPR reduction performance of the I-PTS scheme is similar to that of C-PTS method as an improvement of 0.3 dB was achieved over the original signal. At $CCDF = 10^{-3}$, a PAPR reduction of 1.05 dB is gained by the I-PTS scheme when 16 sub-blocks are employed. Thus, similar to the C-PTS, the simple use of I-PTS in the FBMC signal does not provide better improvement in terms of PAPR suppression despite its low computational complexity over C-PTS.

The results presented in Fig. 6 compare the PAPR performance of the proposed EPTS-IF scheme to the existing C-PTS and I-PTS techniques under 4-OQAM modulation scheme when $N = 64$, $V = 4$ and $W = 2$. The curve FBMC/OQAM indicates the PAPR of the original signal which is approximately 10.5 dB. The CCDF at 10^{-3} shows a PAPR reduction gain of nearly 0.7 dB, and 0.1 dB achieved by the C-PTS compared to the original signal, and I-PTS, respectively. Thus, a slight PAPR reduction improvement can be noticed at the cost of increased computational complexity. After employing the EPTS-IF method, it can be observed that the PAPR decreased by almost 1.7 dB, 1.0 dB, and 1.1 dB compared respectively to the FBMC/OQAM original signal, C-PTS, and I-PTS schemes. Consequently, the EPTS-IF algorithm provides the greatest PAPR reduction performance, and does not involve large complexity.

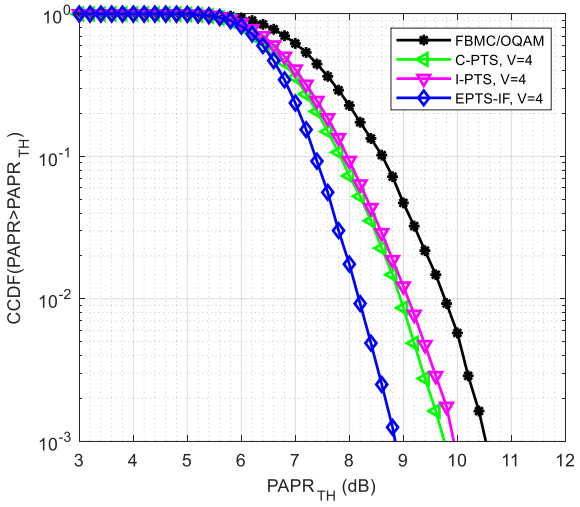

Fig. 6. CCDF vs PAPR performance of the original FBMC/OQAM, C-PTS, I-PTS, and EPTS-IF, $N = 64$, $V = 4$.

Fig. 7 depicts a summary of the results which evaluates the PAPR reduction performance of the proposed PAPR reduction algorithm over the original FBMC signal and the existing PAPR reduction schemes such as C-PTS and I-PTS methods. Simulation has been performed under 4-OQAM modulation, and the parameters N, V and W were set to $64, 8$ and 2, respectively. The simulation results show the PAPRs amount of 10.5 dB, 9.4 dB, and 9.6 dB for the FBMC signal, C-PTS, and I-PTS techniques,

respectively at $CCDF = 10^{-3}$. After applying the EPTS-IF scheme, the PAPR of the original signal decreased to 8.0 dB. This indicates that gains of approximatively 2.5 dB, 1.4 dB, and 1.6 dB are achieved by the EPTS-IF scheme over the original signal, C-PTS, and I-PTS schemes, respectively. This is a valuable achievement especially when realizing that the EPTS-IF employs suboptimal search approach unlike the C-PTS algorithm. Furthermore, compared to the I-PTS, the PAPR performance of the C-PTS experiences an inconsequential improvement of about 0.2 dB as it faces an increase of the computational complexity. Obviously, the proposed method outperforms by far the C-PTS and I-PTS schemes, provides a satisfactory PAPR reduction gain, and involves less complexity.

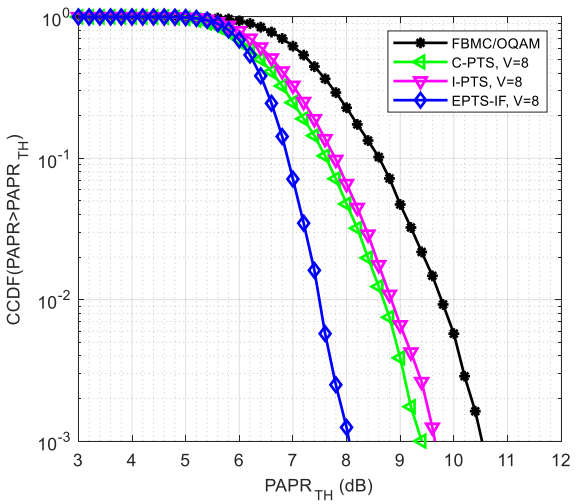

Fig. 7. CCDF vs PAPR performance of the original FBMC/OQAM, C-PTS, I-PTS, and EPTS-IF, $N = 64$, $V = 8$.

Fig. 8 illustrates the PAPR reduction achievement of the EPTS-IF, C-PTS, and I-PTS schemes under simulation parameters such as 16 sub-blocks, 64 subcarriers, and 4-OQAM modulation type. From the depicted results, it can be perceived that the proposed EPTS-IF method provides a remarkable PAPR reduction gain over the C-PTS and I-PTS algorithms. Evaluated at the probability of 10^{-3}, the PAPRs are 7.3 dB, 9.0 dB, 9.45 dB, and 10.5 dB for the EPTS-IF, C-PTS, I-PTS, and original signal, respectively. Over the C-PTS, I-PTS, and FBMC/OQAM signal, the EPTS-IF technique shows an improvement of 1.7 dB, 2.15 dB, and 3.2 dB, respectively. Evidently, the EPTS-IF scheme yields a significant PAPR reduction gain of approximately 30.48% compared to the PAPR of the original signal. Besides, 14.29% of the original PAPR is reduced using the C-PTS algorithm, but at the expense of an exponential complexity. Consequently, the greatest PAPR suppression effect and lowest computational complexity are produced by the proposed EPTS-IF method, while C-PTS and I-PTS schemes yield the worst PAPR reduction performance. In addition of that, it is important to point out that the I-PTS scheme similar to the EPTS-IF does not require high search complexity but exhibits a slight degradation of around 0.45 dB compared with the C-PTS scheme.

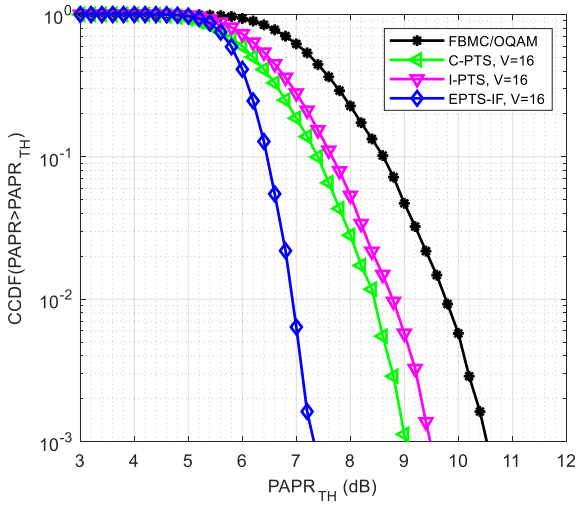

Fig. 8. CCDF vs PAPR performance of the original FBMC/OQAM, C-PTS, I-PTS, and EPTS-IF, $N = 64$, $V = 16$.

The simulation results revealed the ability of the EPTS-IF scheme for significantly reducing the large PAPR for the FBMC/OQAM signals. Besides, the results showed that the existing C-PTS and I-PTS schemes cannot compete with the proposed EPTS-IF scheme in terms of PAPR reduction achievement. However, it is important to recall that the computational complexity aspect has always been one of the key considerations when proposing a PAPR reduction scheme. Thus, relationship between the PAPR values, the number of real addition and multiplication operations for the EPTS-IF, I-PTS, and C-PTS schemes is shown in Table III. Also, the reduced quantity in computational complexity for the proposed EPTS-IF scheme compared to that of the C-PTS was evaluated using the computational complexity reduction ratio (CCRR), given as [31]:

$$CCRR = \left(1 - \frac{Complexity\ of\ the\ EPTS-IF}{Complexity\ of\ the\ C-PTS}\right) \times 100 \qquad (25)$$

B. Discussion

As summarized in Table III, for all the various sizes of sub-blocks ranging from 4 to 16, the proposed EPTS-IF algorithm outperforms undoubtedly both the C-PTS and the I-PTS schemes in terms of high performance PAPR suppression for the FBMC/OQAM signals. Alternatively, the C-PTS scheme produces better PAPR suppression effect compared to the I-PTS method for all sub-block's dimensions; this is due to the use of large space search of phase factor combinations. For $V = 4$, the proposed EPTS-IF scheme decreases the PAPR by nearly 1.0 dB more than the C-PTS, and the number of real multiplication and addition operations involved in the EPTS-IF scheme are as well reduced by 86.11% of that of the C-PTS scheme. When $V = 8$, the C-PTS scheme shows a PAPR reduction performance gain of only 0.4 dB compared to the use of 4 sub-blocks. while the proposed

EPTS-IF scheme upgrades its PAPR suppression gain to 0.8 dB ($V = 8$) in comparison to its prior performance when $V = 4$. Clearly, there is a 1.4 dB gap between the PAPR reduction performance gain achieved by the proposed EPTS-IF and the C-PTS schemes when $V = 8$. Moreover, it can be noticed that the proposed EPTS-IF involves only 1.74% of the number of real multiplication and addition operations involved in the C-PTS scheme. The impact of the number of sub-blocks ($V = 16$) in the PAPR reduction performance of the proposed scheme versus the C-PTS was also simulated. The proposed EPTS-IF scheme yields a PAPR suppression performance gain of around 16.19% over the C-PTS method. Besides, the number of real additions and real multiplications required in the proposed EPTS-IF scheme are practically negligeable compared with that needed in the C-PTS scheme. Thus, from this analysis, it can be stated that besides its ineffectiveness in reducing the PAPR for the FBMC/OQAM signals, the C-PTS scheme exhibits high computational complexity compared to both the proposed EPTS-IF and the I-PTS schemes. Also, the simulation outcomes and analysis show that high PAPR reduction performance with a moderate search complexity could be obtained using the proposed EPTS-IF scheme. Consequently, the proposed EPTS-IF scheme could successfully play a role of low complexity PAPR reduction method for the FBMC/OQAM signals.

TABLE III: COMPUTATIONAL COMPLEXITY COMPARISON IN TERMS OF REAL MULTIPLICATION AND ADDITION OPERATIONS

Method	**Real multiplications**			**Real additions**			**PAPR** at $CCDF = 10^{-3}$		
	$V = 4$	$V = 8$	$V = 16$	$V = 4$	$V = 8$	$V = 16$	$V = 4$	$V = 8$	$V = 16$
EPTS-IF	327680	1310720	5242880	286720	1228800	5079040	8.8	8.0	7.3
I-PTS	1179648	4718592	18874368	1032192	4423680	18284544	9.9	9.6	9.45
C-PTS	2359296	75497472	38654705664	2064384	70778880	37446746112	9.8	9.4	9.0
CCRR (%)	86.11	98.26	99.98	86.11	98.26	99.98			

V. CONCLUSIONS AND FUTURE WORKS

In this paper, a PAPR reduction scheme was proposed in the interest of reducing the high PAPR in the FBMC/OQAM system. The FBMC/OQAM data blocks were partitioned into sub-blocks and then buffered with consideration of the overlaps between them. Next, the overall partitioned data blocks were divided into several segments of sub-blocks which were later individually optimized using a suboptimal combinatorial search approach. Results from computer simulation and analysis reveal that the proposed scheme is practical and efficient in reducing the PAPR for the FBMC/OQAM signals, and could provide a substantial PAPR reduction performance. Furthermore, the proposed EPTS-IF scheme by far outperforms both the C-PTS and I-PTS methods in terms of PAPR reduction performance gain, and involves much less computational complexity. Hence, the proposed EPTS-IF scheme is a very feasible PAPR minimization method that could appropriately be employed for the FBMC/OQAM signals. This paper considered iterative flipping method in optimizing the phase rotation factors for PAPR reduction in FBMC/OQAM systems. However, as future work, other optimization techniques including iterative local search and simulated annealing will be investigated to optimize the phase factors so as to minimize the high PAPR for FBMC/OQAM signal. Moreover, as the complexity in iterative flipping approach could grow when large number of flipped bits are employed, the computational complexity reduction will be considered in future work as well.

CONFLICT OF INTEREST

The authors declare no conflict of interest.

AUTHOR CONTRIBUTIONS

Mahaman Noura Issaka Ango conducted the research, performed the analysis and interpretation of results; contributed reagents, materials, analysis tools and wrote the manuscript. Elijah Mwangi contributed design the experiment, reagents, and reviewed the results. Moctar Mossi contributed reagents, and reviewed the results.

REFERENCES

[1] S. Sidiq, J. A. Sheikh, F. Mustafa, B. A. Malik, and I. B. Sofi, "PAPR Minimization of FBMC/OQAM scheme by hybrid SLM and PTS using artificial: Bee-Colony Phase—Optimization," *Arab. J. Sci. Eng.*, vol. 46, pp. 9925-9934, Apr. 2021.

[2] A. E. Agoni, M. Dlodlo, and H. O. Ohize, "Capacity analysis of FBMC over OFDM in cognitive radio systems," in *Proc. IEEE Global Wireless Summit (GWS)*, Cape Town, South Africa, 2017, pp. 52–56.

[3] B. Khan and F. J. Velez, "Multicarrier waveform candidates for beyond 5G," in *Proc. IEEE 12th International Symposium on Communication Systems, Networks and Digital Signal Processing (CSNDSP)*, Porto, Portugal, 2020, pp. 1–5.

[4] M. Shaik and R. S. Yarrabothu, "Comparative study of FBMC-OQAM and OFDM communication system," in

Proc. IEEE 2nd International Conference on Trends in Electronics and Informatics (ICOEI), Tirunelveli, India, 2018, pp. 559–563.

[5] H. M. Abdel-Atty, W. A. Raslan, and A. T. Khalil, "Evaluation and analysis of FBMC/OQAM systems based on pulse shaping filters," *IEEE Access*, vol. 8, pp. 55750–55772, Mar. 2020.

[6] M. C. P. Paredes, F. Grijalva, J. Carvajal-rodr, and F. Sarzosa, "Performance analysis of the effects caused by HPA models on an OFDM signal with high PAPR," in *Proc. IEEE Second Ecuador Technical Chapters Meeting (ETCM)*, Salinas, Ecuador, 2017, pp. 1–5.

[7] Y. A. Jawhar, *et al*., "A review of partial transmit sequence for PAPR reduction in the OFDM systems," *IEEE Access*, vol. 7, pp. 18021–18041, Feb. 2019.

[8] L. Dang, H. Li, and S. Guo, "Constellation Extension and Hadamard Transform," in *Proc. IEEE 13th International Conference on Intelligent Computer Communication and Processing (ICCP)*, Cluj-Napoca, Romania, 2017, pp. 543–549.

[9] M. Ali, R. K. Rao, and V. Parsa, "PAPR reduction in OFDM systems using clipping based on symbol statistics," in *Proc. IEEE 30th Canadian Conference on Electrical and Computer Engineering (CCECE)*, Windsor, Canada, 2017, pp. 2–6.

[10] X. Liu, X. Zhang, and J. U. N. Xiong, "An enhanced iterative clipping and filtering method using time-domain kernel matrix for PAPR Reduction in OFDM Systems," *IEEE Access*, vol. 7, pp. 59466–59476, May. 2019.

[11] K. Yadav and C. Srinivasarao, "PAPR reduction of OFDM signals using a nonlinear transform method," in *Proc. International Conference on Wireless Communications, Signal Processing and Networking (WiSPNET)*, Chennai, India, 2017, pp. 325–328.

[12] R. Musabe, *et al*., "PAPR reduction in LTE network using both peak windowing and clipping techniques," *Journal of Electrical Systems and Inf Technol.*, vol. 6, no. 3, pp. 1–11, Nov. 2019.

[13] A. Idris, N. L. M. Sapari, M. S. Idris, S. S. Sarnin, W. N. W. Mohamad, and N. F. Naim, "Reduction of PAPR using block coding method and APSK modulation techniques for F-OFDM in 5G system," in *Proc. TENCON 2018 - IEEE Region 10 Conference*, Jeju, Korea (South), 2018, pp. 2456–2460.

[14] C. Hu, L. Wang, and Z. Zhou, "A modified SLM scheme for PAPR reduction in OFDM systems," in *Proc. IEEE 10th International Conference on Electronics Information and Emergency Communication (ICEIEC)*, Beijing, China, 2020, pp. 61–64.

[15] L. J. Cimini and N. R. Sollenberger, "Peak-to-Average power ratio reduction of an OFDM signal using partial transmit sequences," in *Proc. IEEE International Conference on Communications*, Vancouver, BC, Canada, 1999, pp. 511–515.

[16] B. Cai, A. Liu, X. Liang, and F. Cheng, "A class of PAPR reduction methods for OFDM signals using partial transmit sequence," in *Proc. IEEE 8th Joint International Information Technology and Artificial Intelligence Conference (ITAIC)*, Chongqing, Chin, 2019, pp. 861–865.

[17] B. Wang, Q. Si, and M. Jin, "A novel tone reservation scheme based on deep learning for PAPR reduction in OFDM systems," *IEEE Commun. Lett.*, vol. 24, no. 6, pp. 1271–1274, Jun. 2020.

[18] S. Ikni, D. Abed, S. Redadaa, and M. Sedraoui, "PAPR reduction in FBMC-OQAM systems based on discrete sliding norm transform technique," *Radioelectron. Commun. Syst.*, vol. 62, pp. 51–60, Apr. 2019.

[19] S. Senhadji, Y. M. Bendimerad, and F. T. Bendimerad, "New scheme for PAPR reduction in FBMC-OQAM systems based on combining TR and deep clipping techniques," *International Journal of Electrical and Computer Engineering (IJECE).*, vol. 11, no. 3, pp. 2143–2152, 2021.

[20] H. Wang, "A hybrid PAPR reduction method based on SLM and multi-data block PTS for FBMC/OQAM systems," *Information*, vol. 9, no. 10, pp. 246–257, Oct. 2018.

[21] V. S. Kumar, "Joint Iterative filtering and companding parameter optimization for PAPR reduction of OFDM/OQAM signal," *AEUE-International Journal of Electronics and Communications.*, vol. 124, pp. 153365–153371, Sep. 2020.

[22] A. Hanprasitkum, A. Numsomran, P. Boonsrimuang, and P. Boonsrimuang, "Improved PTS method with new weighting factor technique for FBMC-OQAM systems," in *Proc. 19th International Conference on Advanced Communication Technology (ICACT)*, PyeongChang, Korea (South), 2017, pp. 143–147.

[23] S. Ni, M. Lei, M. Zhao, and M. Lit, "Improved PTS Technique for the PAPR-Reduction of FBMC-OQAM Signals," in *Proc. IEEE 88th Vehicular Technology Conference (VTC-Fall)*, Chicago, IL, USA, 2018, pp. 1–5.

[24] J. H. Moon, Y. R. Nam, and J. H. Kim, "PAPR reduction in the FBMC-OQAM system via segment-based optimization," *IEEE Access*, vol. 6, pp. 4994–5002, Jan. 2018.

[25] H. Merah, Y. Merrad, M. H. Habaebi, and M. Mesri, "A novel PTS-based PAPR reduction scheme for FBMC-OQAM system without extra bit transmission of SI," *International Journal of Electronics.*, vol. 108, no. 6, pp. 928–944, 2021.

[26] C. Xing, *et al*., "A novel conversion vector-based low-complexity SLM scheme for PAPR reduction in FBMC/OQAM systems," *IEEE Trans. Broadcast.*, vol. 66, no. 3, pp. 656–666, Sep. 2020.

[27] S. Lv, J. Zhao, L. Yang, and Q. Li, "Genetic algorithm based bilayer PTS scheme for peak-to-average power ratio reduction of FBMC/OQAM signal," *IEEE Access*, vol. 8, pp. 17945–17955, Jan. 2020.

[28] L. Yao, E. Wang, and X. Peng, "Design and research on FBMC-OQAM multicarrier technology for 5G," in *Proc. International Conference on Advanced Algorithms and Control Engineering (ICAACE)*, 2019, pp. 1–7.

[29] A. Viholainen, B. Bellanger, and M. Huchard. (2009). PHYDYAS – PHYsical layer for DYnamic Access and cognitive radio. [Online]. Available: http://www.ict-

phydyas.org/delivrables.
[30] D. Qu, S. Lu, and T. Jiang, "Multi-block joint optimization for the peak-to-average power ratio reduction of FBMC-OQAM signals," *IEEE Trans. Signal Process.*, vol. 61, no. 7, pp. 1605–1613, Apr. 2013.
[31] M. S. Ahmed, S. Boussakta, A. Al-Dweik, B. Sharif, and C. C. Tsimenidis, "Efficient design of selective mapping and partial transmit sequence using T-OFDM," *IEEE Trans. Veh. Technol.*, vol. 69, no. 3, pp. 2636–2648, Mar. 2019.

Mahaman Noura was born in Akokan, Niger in 1992. He received the B.Sc. degree in electrical, and electronics engineering from Université Abdou Moumouni, Niamey, Niger, in 2016. He is currently pursuing the M.Sc. degree in electrical engineering (telecommunication-option) in the Pan African University, Nairobi, Kenya. His current research interests include digital signal processing for wireless communication, FBMC and PAPR reduction in multicarrier systems.

Elijah Mwangi received the B.Sc. and M.Sc. degrees in electrical and electronic engineering from University of Nairobi, Nairobi, Kenya, in 1978 and 1983, respectively. He obtained the Ph.D. degree in electrical and electronic engineering from Loughborough University of Technology, Loughborough, UK, in 1987. Since 1981, he has been with the faculty of Engineering at University of Nairobi, Nairobi, Kenya, where he is currently a Professor. His current research interests comprise digital image processing, digital signal processing, OFDM and PAPR reduction in multicarrier systems.

Moctar Mossi received the M.Sc. degree in signal processing from University of Rennes 1, Rennes, France, in 2008. He obtained the Ph.D. degree in signal processing and automatic control engineering from University of Nice-Sophia-Antipolis, Nice, France, in 2012. Since 2018, he has been a Research Assistant and lecturer in the Physics Department at Université Abdou Moumouni, Niamey, Niger. His research interests include signal processing and control engineering. He is a member of IEEE.